Materials Research Bulletin 159 (2023) 112105

Contents lists available at ScienceDirect

Materials Research Bulletin

journal homepage: www.elsevier.com/locate/matresbu

Research Papers

Dielectric and transient electrical response of SmB_6 single crystals

Jolanta Stankiewicz [*,a], Pedro Schlottmann [b], Javier Blasco [c], Monica Ciomaga Hatnean [d], Geetha Balakrishnan [d]

[a] Departamento de Física de la Materia Condensada, Universidad de Zaragoza, Zaragoza 50009, Spain
[b] Department of Physics, Florida State University, Tallahassee, FL 32306, USA
[c] Instituto de Ciencia de Materiales de Aragón and Departamento de Física de la Materia Condensada, CSIC–Universidad de Zaragoza, Zaragoza 50009, Spain
[d] Department of Physics, University of Warwick, Gibbet Hill Road, Coventry CV4 7AL, UK

ARTICLE INFO

Keywords:
Samarium hexaboride
Impedance spectroscopy
Current–controlled voltage oscillations

ABSTRACT

We report results from an in–plane and out–of–plane impedance study on SmB_6 single crystals, performed at low temperatures and over a wide frequency range. A universal equivalent circuit describes the dielectric behavior of this system across the transition, from surface to bulk dominated electrical conduction between 2 and 10 K. We identify the resistive, capacitive, and inductive contributions to the impedance. The equivalent inductance, obtained from fits to experimental data, drops drastically with increasing temperature, as the bulk starts to control electrical conduction. Self–sustained voltage oscillations, observed below 6 K across small crystals when biased with a *dc* current, point to a large SmB_6 self–capacitance, likely brought by the surface states.

1. Introduction

SmB_6 is a strongly correlated Kondo insulator that was recently found to have a robust surface state. It shows high–temperature metallic behavior which changes to an insulating one below 40 K as an energy gap $\Delta \approx 15$–20 meV opens. This energy gap, brought in by hybridization between the localized Sm 4*f* states and weakly correlated (mostly) Sm 5*d* states, should lead to a diverging resistance at lower temperatures. Instead, the resistance flattens below 5 K, which imply a metallic surface state. The concept of a tofpological insulator (TI) [1], i.e., a material that has an insulating bulk with non–trivial topological protected surface states, was invoked as a likely explanation for the low–temperature resistance saturation of SmB_6 [2–10].

Most of the recent experimental research on SmB_6 shows conclusively that metallic surface conduction lies behind the leveling–off of its low–temperature resistivity. However, some results (e.g. specific heat, optical conductivity and quantum oscillation measurements) indicate a bulk origin of SmB_6 metal–like behavior at low temperatures [11–13]. There is currently no clear consensus on this point. The correlated state of SmB_6 seems only slightly affected by disorder or light doping with non–magnetic impurities [14,15]. All these features make SmB_6 an attractive candidate for applications.

Most of research on this system has been focused on its equilibrium properties. However, samarium hexaboride shows interesting transient behavior which is not well studied. A large nonlinear resistance and an oscillating response upon biasing single crystals with a small *dc* current at low temperatures are two examples of such transient phenomena [16]. A model which involves both surface and bulk states, in addition to a strong coupling between the thermal and the electrical properties, has recently been put forward to explain this response [17]. Nevertheless, there are only few reports on the frequency–dependent transport properties of SmB_6.

Here, we report results from impedance spectroscopy (IS) experiments on SmB_6, performed at low temperatures and over a wide frequency range. By applying a single frequency voltage to the sample, the phase shift and amplitude of the resultant current can be determined. Both the magnitude (resistive) and phase shift (reactive) component of a frequency–dependent impedance yield relevant information about intrinsic and extrinsic dielectric relaxation processes. In a linear approach, the total response of the system can be described by inductive, capacitive, and resistive elements of an equivalent electrical network. These components are uniquely defined and give clear and simple description of the underlying physical processes involved. We focus our study on the 2 to 10 K temperature range in which the SmB_6 system shows a nontrivial behavior with topological–surface and bulk conduction channels competing. In addition, we pursue nonlinear dynamics in this region, where large self–sustained voltage oscillations appear across reduced SmB_6 crystals biased with a small *dc* current.

* Corresponding author.
E-mail address: jolanta@unizar.es (J. Stankiewicz).

https://doi.org/10.1016/j.materresbull.2022.112105
Received 31 May 2022; Received in revised form 23 September 2022; Accepted 13 November 2022
Available online 16 November 2022

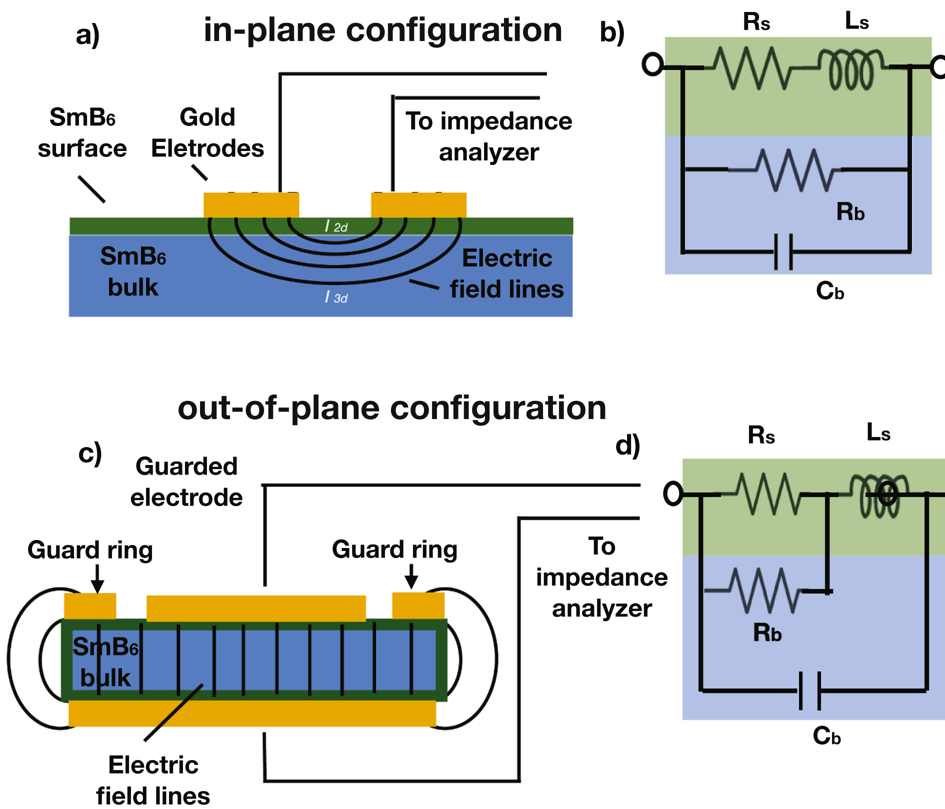

Fig. 1. (Color online))(a) Measurement setup for in–plane impedance spectroscopy of a SmB_6 single crystal in the frequency range from 20 Hz to 10 MHz and between 2 and 300 K. (b) Equivalent circuit of the device. (c) Set-up for out–of-plane impedance measurements. (d) Equivalent circuit of the device. R_bC_b parallel connection models the insulating bulk contribution to the total impedance, whereas the R_sL_s branch gives the inductive response from the sample surface.

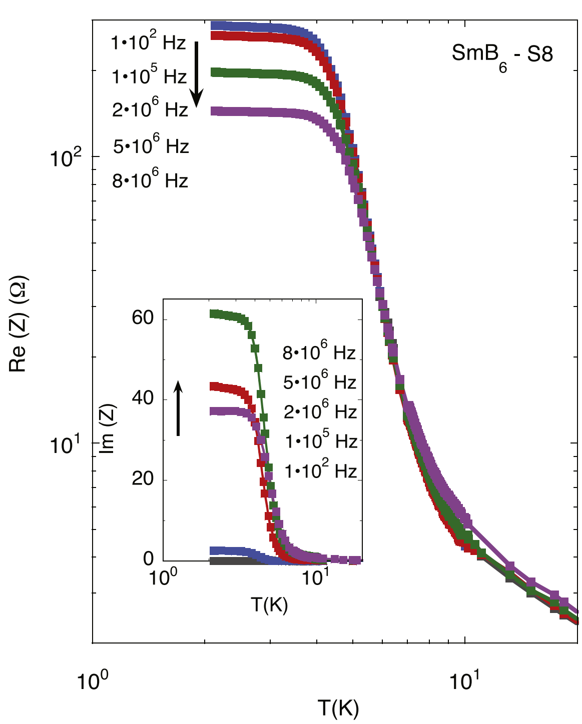

Fig. 2. (Color online) Real part of the in-plane impedance for single crystal SmB_6 (sample S8) vs. temperature. The inset shows the imaginary part of the impedance vs. temperature for the same crystal.

The remainder of the paper is as follows. The experimental procedure is described in Section II. Results of measurements are reported and discussed in Section III, and conclusions are drawn in Section IV.

2. Experiment

Ac impedance measurements on stoichiometric SmB_6 single crystals were carried out in the 1.8 to 300 K temperature range using a Quantum Design physical properties measurement system (PPMS). SmB_6 crystals were grown by the floating zone technique using a high power xenon–arc–lamp–image furnace. This method yields large single crystals free of contamination although vacancies and defects might be still present [18]. Samples used in the experiments were selected from a batch of samples based on their quality and size. The surfaces of these crystals, (100 planes), were carefully etched, using a mixture of hydrochloric acid and water, to remove possible oxide layers. We used silver paint, gold or pure indium to prepare contacts for impedance measurements, on recently cleaved, about 200 μm thick samples. We did not observe any important features in our measurements which could be related to contacts we have applied.

Impedance spectra were obtained with a precision impedance analyzer (Wayne-Kerr) in the 20 Hz up to 10 MHz frequency range. An excitation amplitude of 0.01V was applied to ensure the ohmic regime with a low signal–to–noise ratio. Before connecting the sample, open–circuit and short–circuit tests, in addition to high frequency compensation were carried out, to minimize parasitic contributions from the measurement setup. IS measurements were performed in both out–of plane and in–plane configurations shown in Fig. 1. In former configuration, a parallel plate capacitor configuration, stray capacitance may form on the edges of the electrodes. This causes a measurement error that can be avoided using the guard electrode which absorbs the electric field at the edge. We applied this guarded method in out–of plane studies

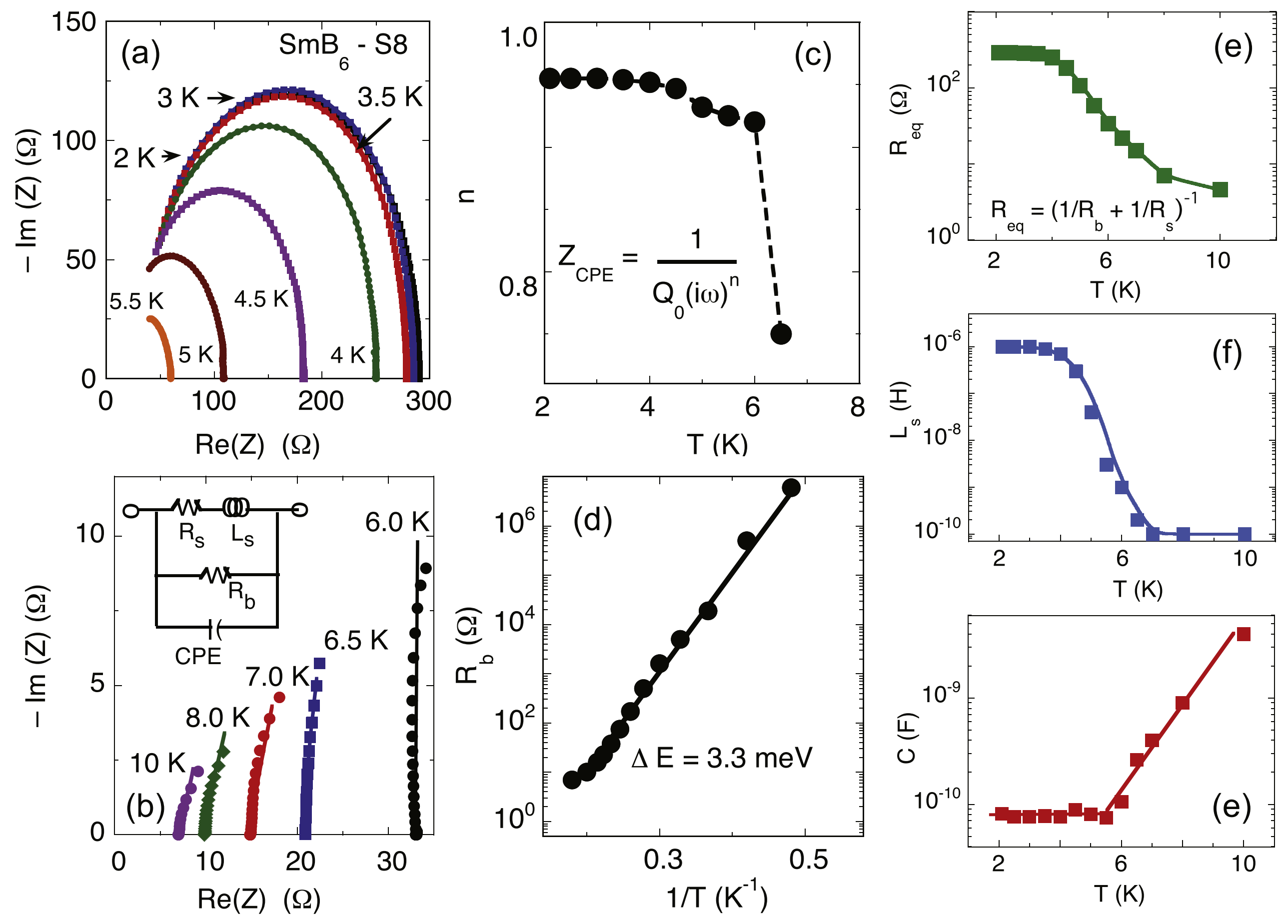

Fig. 3. (Color online) (a) and (b) - IS data for $T \leq 10$ K, plotted as the negative imaginary part vs. real part of the impedance (Cole-Cole plot) for SmB_6 crystal (sample S8). Symbols indicate the data; solid lines represent the fit of the data to the model shown in Fig. 1 (b). (c) - variation of the constant phase element exponent n with temperature. (d) through (g) - fitted temperature dependences of the equivalent circuit elements for SmB_6 (sample S8): (d) - R_b as a function of $1/T$. (e) R_{eq}, as defined in the figure. (f) Inductance L_s, showing a large drop between 4 and 6 K. (g) Capacitance C_b.

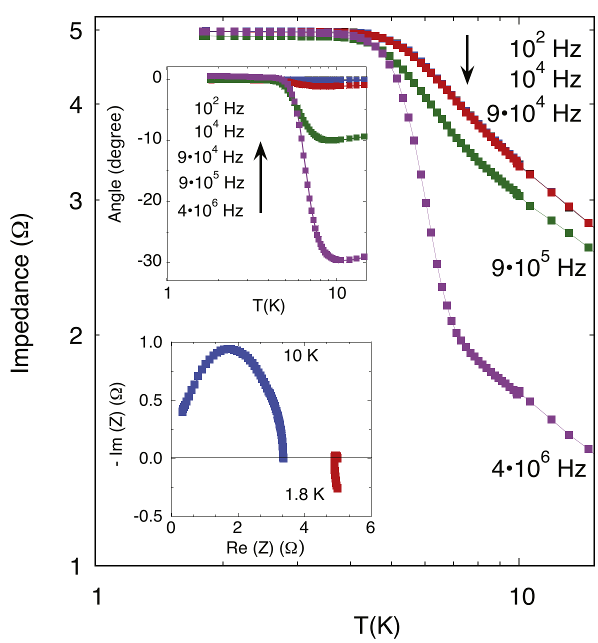

Fig. 4. (Color online) In-plane impedance for single crystal SmB_6 (sample S9) as a function of temperature at various frequencies. The upper inset shows phase angle vs. temperature. The lower inset displays the Cole–Cole plot at 1.8 and 10 K for the same sample. Note that $Im(Z)$ is positive at 1.8 K.

(see Fig. 1 c). On the other hand, for an in–plane configuration, reducing the electrode spacing diminishes the proportion of the current carried through the bulk and increases the measurement sensitivity to the surface properties (see Fig. 1 a).

To complete our study, current–voltage ($I - V$) characteristics were measured at low temperatures. The SmB_6 samples can be driven into a dissipative regime with increasing current below about 6 K, where the $I - V$ relation shows nonlinear negative differential resistance (NDR) from self heating. To properly measure temperature changes arising from current flow, we used a differential chromel vs. Au-0.07 at.% Fe thermocouple between the cryostat base and the top of the sample. In addition, we monitor voltage self–induced oscillations seen in several crystals upon biasing with a small *dc* current at low temperatures.

3. Results and Discussion

3.1. Impedance spectroscopy

We analyze the dielectric response of SmB_6 single crystals in the complex plane. To exclude extrinsic contributions, this is done for different types of contacts and sample geometries. Interpretation of results is carried out in terms of electronic networks to ensure that the observed variations of complex impedance arise from an intrinsic mechanism. In Fig. 2, we plot the real $Re(Z)$ and imaginary $Im(Z)$ part of impedance Z for a single crystalline SmB_6 (sample S8) as a function of temperature T, in the range from 2 to 20 K, for various frequencies. These data have been obtained for the in-plane configuration, with a

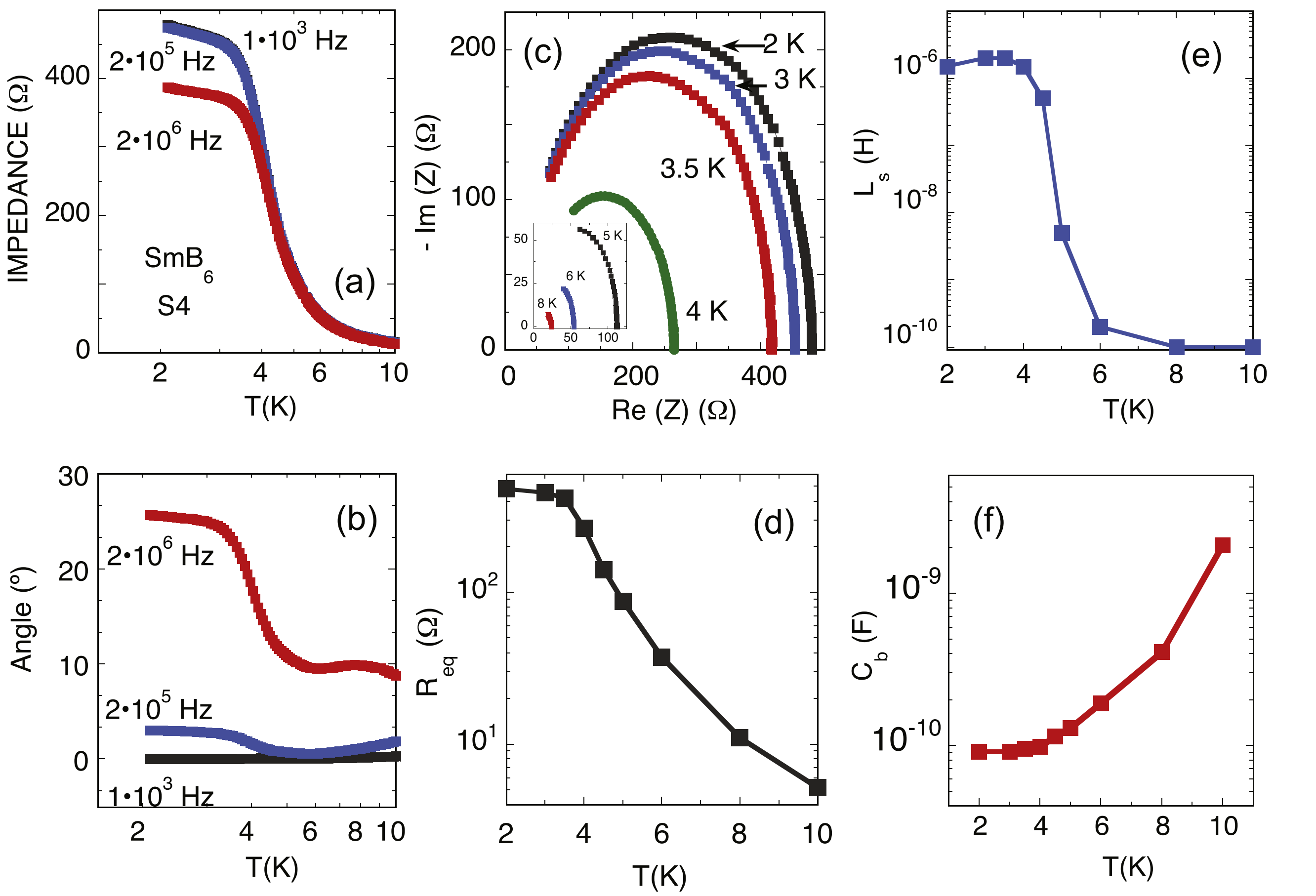

Fig. 5. (Color online) (a)- Guarded out-of plane impedance for single crystal SmB_6 (sample S4) as a function of temperature at various frequencies. (b)- Phase angle *vs.* temperature for the same sample. (c)- Cole–Cole plot between 2 and 10 K. (d)- R_{eq}, obtained from the fit to the equivalent circuit vs. T. (e)- Values of the fitted inductance L_s, and (f)- capacitance C_b as a function of T.

probe separation of approximately 150 μm (see Fig. 1(a)). Upon lowering the temperature, $Re(Z)$ starts to increase quite sharply at about 20 K and levels out below $T \lesssim 5$ K. Previous studies of high quality SmB_6 single crystals have shown the evolution of this system from a semi-metallic state at room temperature to a Kondo correlated insulating state, and finally to a very low carrier density metallic state at low temperatures. It is now generally accepted that, for $T \lesssim 5$ K, the transport in SmB_6 takes place through surface states (SS), as the bulk resistance R_b is much higher than the surface resistance R_s. With increasing temperature ($4 \lesssim T \lesssim 10$ K), R_b becomes comparable to that of the SSs, and conduction proceeds through both the bulk of the crystal and the surface channels. Beyond 10 K and up to approximately 40 K, the bulk resistance over this temperature range is much smaller than that of the surface states, and the latter have no effect on electrical transport. The data plotted in Fig. 2 follow this scheme. Assuming that the surface conductivity is independent of temperature, we obtain for the bulk resistance a thermally activated behavior $R_b \propto \exp(\Delta E / k_B T)$, with an activation energy of 3.3 meV, for 2 K$< T <$10 K.

The imaginary part of $Z(T)$ for the sample S8 also shows a pronounced rise below 5 K for large excitation frequencies, followed by leveling out at lower temperatures (see inset in Fig. 2). The Kondo insulator SmB_6 appears to have an intrinsic metal to high-dielectric material transition. As its insulating gap opens completely at low temperatures, the bulk becomes an insulator with a large dielectric constant, whereas the surface states are metallic. This can be represented by an equivalent parallel RC circuit and a topological surface state [1].

Fig. 3(a) and (b) show the IS data plotted as the negative imaginary $-Im(Z)$ vs. the real part $Re(Z)$ (Cole–Cole plot) at various temperatures in the range from 2 to 10 K. In such impedance plots, one or more semicircles may be seen for a parallel resistor-capacitor RC circuit measurement; each semicircle corresponding to dielectric relaxation arising from different, extrinsic (interfaces) or intrinsic (sample), contributions in series [20]. Our data show one single, “non-ideal” dielectric relaxation, evidenced by one depressed semicircle for each temperature, where the centre of each semicircle has shifted below the x-axis ($Re(Z)$). For a Debye–like relaxation (an ideal parallel resistor-capacitor element), a perfect semicircle is expected [21]. Since the data cannot be modeled solely using standard RC elements, we used the alternative equivalent circuit depicted in Fig. 1(b), which yields good fits at all frequencies. The “depressed” behavior can be fitted by adding a series R_sL_s branch, in parallel to the conventional RC element. Physically, the R_bC_b part accounts for the insulating SmB_6 bulk, with a standard dielectric behavior (Fig. 1(b)). The R_sL_s branch corresponds to the inductive response, most likely from the sample surface. We also examined the equivalent circuit, displayed in the inset of Fig. 3(b) [21], which gives a somewhat better fit for the sample S8 data. The Constant Phase Element (CPE) has an impedance of the form $Z(CPE) = 1/(Q_o(i\omega)^n)$ where Q_o models the effects of a non-ideal relaxation process or retardation. The exponent n is a measure of the “non-ideality” of the relaxation process, brought about by non-uniformity of physical properties of the system. When $n = 1$, the system is described by a single time-constant and the parameter Q_o has units of capacitance. Its variation with T, obtained from fittings to the circuit in the inset of Fig. 3(b), is shown in Fig. 3(c).

The fitting parameters we have extracted from our model for the S8 sample are shown in Fig. 3 (d)–(g), where each point on the curves

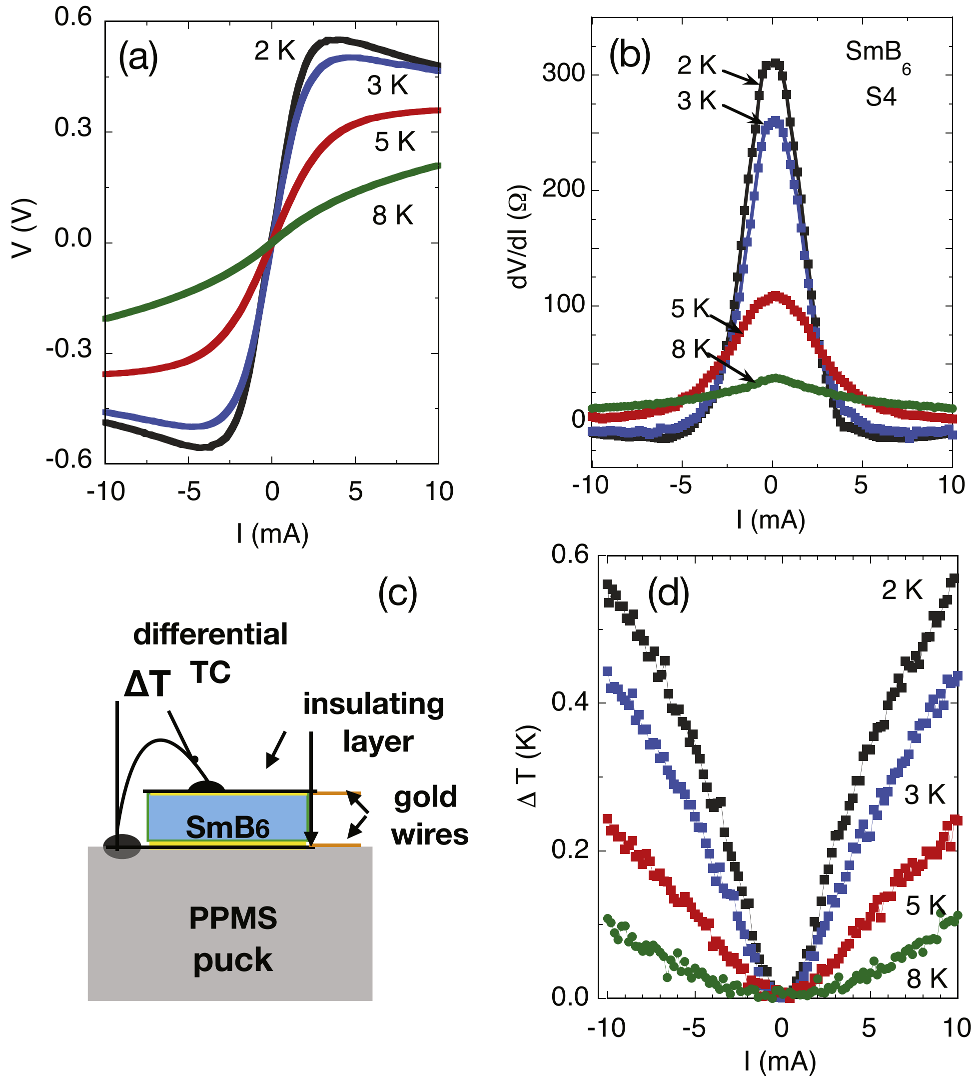

Fig. 6. (Color online)(a)- $I-V$ curves for single crystal SmB_6 (sample S4) at various temperatures. (b)- dV/dI curves at the same temperatures. (c)- set–up used to measure ΔT. (d)- self heating effect of *dc* current (ΔT *vs.* I) measured for the same sample.

represents a fit at a specific temperature. For this sample, $R_s = 288.5\Omega$. As discussed above, the bulk resistance R_b follows thermally activated behavior with an activation energy of 3.3 meV for 2 K< T <10 K. The equivalent sample resistance R_{eq} is calculated as $(1/R_b + 1/R_s)^{-1}$. It is worth noticing that R_b and R_{eq} are very close above 6 K, suggesting that the current flows mainly through bulk beyond this temperature. Fig. 3 (g) depicts the sample capacitance C_b we have estimated from the model. The capacitance stays constant as the temperature increases up to about 6 K, where it upturns. For the in-plane configuration (see Fig. 1 (a)), the field lines of the applied *ac* electric field are not parallel in the sample and the changes in capacitance may not necessarily reflect intrinsic changes in the bulk dielectric permittivity. Fig. 3(f) shows temperature variation of fitted values for the inductance L_s. In the low–temperature metallic state below 4K, $L_s \approx 10^{-6}$ H. As the temperature increases, L_s drops by four orders of magnitude between 4 and 6 K, and is negligibly small farther on. We note that the temperature variations of L_s and R_{eq} are alike in the temperature range considered. The large drop of L_s occurs at the transition from surface to bulk dominated conduction. The inductive contribution in the metallic regime may arise from the coupling of 2D (metallic) and 3D (bulk) conduction channels, likely through defects [22]. The floating zone crystals used in this study tend to host more dislocations and vacancies than the SmB_6 crystals grown from Al flux. In addition, a recent scanning microwave impedance microscopy study uncovers one–dimensional conducting states in SmB_6 which terminate at surface step edges [23]. Such unconventional conduction channels might as well lead to large inductance.

The IS data for SmB_6 (sample S9) are reported in Fig. 4. This sample is identical to the S8 sample, except for the contact separation (approximately 25 μm) which is almost one order of magnitude smaller than in sample S8. Therefore, we expect surface effects to be more pronounced. Indeed, the total impedance increase at high frequencies shows behaviour typical of inductive contributions. The imaginary impedance $Im(Z)$ is then positive at 1.8 K because the spectra are dominated by the surface inductance L_s. The model applies just the same.

The IS results obtained for the out-of plane configuration (see Fig. 1 (b)) of SmB_6 single crystals (samples S1–S4) are much the same as the results for in-plane configuration. Fig. 5(c) shows the Nyquist plot for sample S4 at several temperatures in the range 2 K-10 K. Variations of the magnitude of the impedance $Z(T)$ and of the phase angle $\theta(T)$ at various frequencies are displayed in Fig. 5(a) and (b). The values of the parameters, obtained from the fit to the equivalent circuit of Fig. 1, are plotted in Fig. 5(d)–(f). As discussed above, the inductive contribution is important below 4 K, drops by several orders of magnitude with increasing temperature and becomes negligible beyond 6 K.

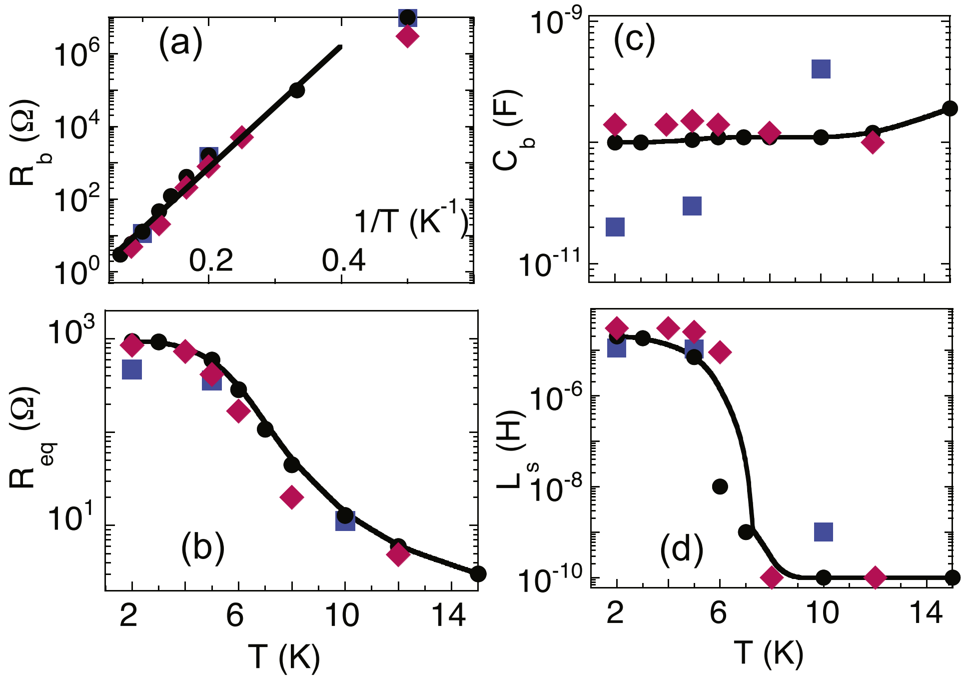

Fig. 7. (Color online) Values of the equivalent circuit elements, obtained from impedance spectra, for SmB_6 samples (black filled circles for S10, blue filled squares for S11, and red filled diamonds for S12, respectively): (a) - R_b as a function of $1/T$. (b) - R_{eq} as a function of T, (c) - C_b, and (d) - inductance L_s variation with T. (For interpretation of the references to colour in this figure legend, the reader is referred to the web version of this article.)

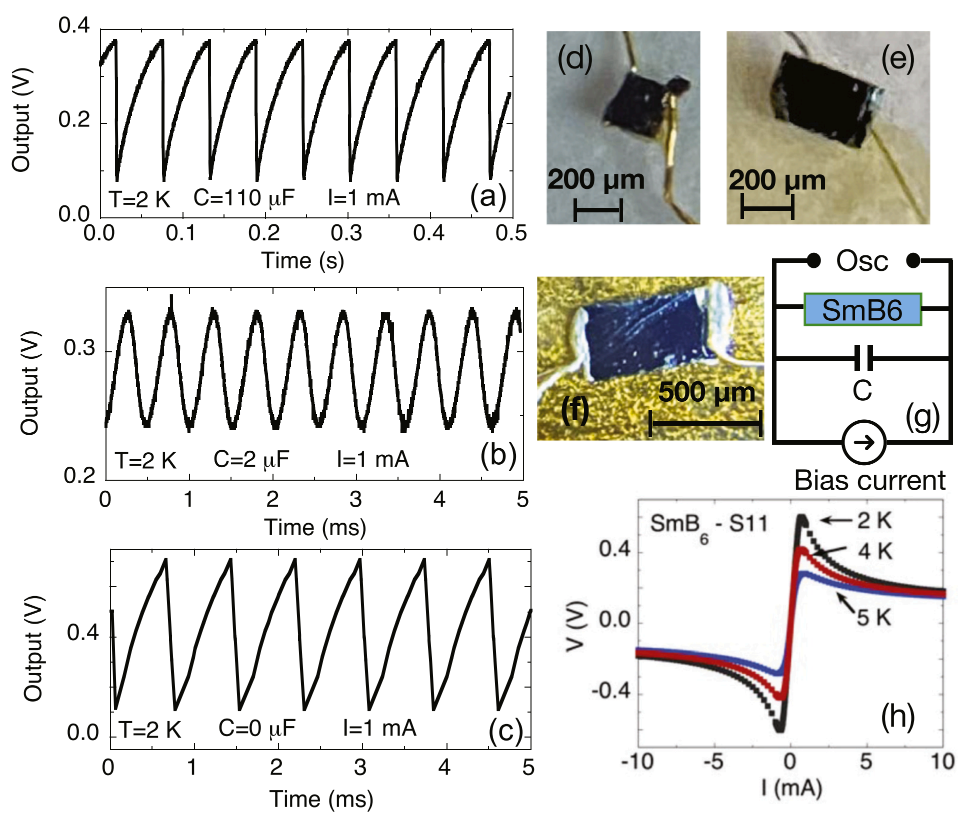

Fig. 8. (Color online) (a)–(c) Oscillation outputs with a dc bias current of 1 mA for three SmB_6 crystals whose images are shown in (d)–(f). The outputs are measured by an oscilloscope using a circuit drawn in (g). No external capacitors C are needed to observe oscillations for the samples in (d) and (f). (h)- $I-V$ curves for sample S-11 (image in (d)) at various temperatures.

Our fits to experimental data were carried out with the least–square method. The relative error in parameters L_s and C_b is less than 5% for $T \lesssim 5$ K. However, for $T \geq 6K$, the fitting parameters may be more uncertain because of the small signal measured. In addition, we observe some parasitic stray inductance for the sample S8 (in–plane configuration) which bends curves in the Cole–Cole plot very slightly to the right for $T \geq 6K$. Since any contribution to the impedance from the experimental setup (wires plus apparatus) should be temperature independent, this is brought, most likely, by electrodes.

3.2. Nonlinear negative differential resistance

Current-voltage characteristics for SmB_6 samples show nonlinear negative differential resistance (NDR) below about 5 K when biased with a small *dc* current. Fig. 6(a) and (b) exhibit $I - V$ and dV/dI plots for sample S4 at various temperatures. Fig. 6(d) displays the corresponding change in sample temperature. The observed increment in temperature, ΔT, is less than 0.6 K over the base temperature of 2 K.

The NDR is brought about by self heating in SmB_6 crystals. Similar behavior, albeit with a larger ΔT for SmB_6 single crystals, has been reported in Ref. [16]. In addition, the authors of this report find large voltage oscillations driven by a small *dc* current. To account for this, a model, in which a coupling between metallic surface conduction and thermally activated bulk conduction gives rise to a large variation in sample heating, was proposed [17]. Qualitatively, the Joule heating in the surface conduction regime rises locally the sample temperature. As a result, the sample resistance decreases, enabling bulk conduction, and thus reducing Joule self heating. Consequently, the sample temperature drops to the initial value and drives the system back to the surface conduction regime. This model, for a rather narrow range of the parameters, yields voltage oscillations that agree with experiment.

In our impedance set–up, we do not find self-sustained oscillations in the SmB_6 crystals. The dynamics of the model reported in Ref. [17] depends importantly on the ratio of the bulk resistance to the surface resistance in thermal equilibrium. This ratio is about or less than 80 in the crystals of Refs. [16,17,24], whereas it is larger than 10^4 for SmB_6 we have studied. As a result, raising the sample temperature by 1 K in the former case (from a base temperature of 2 K) is sufficient to drive SmB_6 crystals into a bulk conduction regime but our samples must be heated at least 5 K in order to reach the same conduction regime. On this account, the sample heating upon biasing with a *dc* current is much smaller in the impedance experiments. In addition, the model of Ref. [17] involves local effects and it is not known which portion of the sample is affected by current. It is not so in the experimental configuration we have used in which the whole sample is subjected to heating. These features might have hindered the non-linear oscillations found in Ref. [17].

Nevertheless, we observe self-sustained oscillations in the SmB_6 contacted by micro-spot-welded 25 μm gold wires or by pure indium deposited on crystal edges. Impedance spectra of these samples yield values of the equivalent circuit elements which are plotted in Fig. 7 for the temperature range from 2 K to 15 K. Their overall variation with T is much the same as in crystals reported above although we find larger values of the surface resistance and the inductance L_s for these samples as expected because of their larger surface area (see Supplementary Material) [19].

Fig. 8 shows spontaneous voltage self–oscillations across three single crystals of SmB_6 upon biasing with a small constant current at 2 K. The images of the contacted samples are displayed in Fig. 8(d) to (f) and the circuit used is drawn in (g). The bias current corresponds to the NDR region of the $I - V$ curves, one of which is plotted in Fig. 8(h). The voltage oscillations developed across SmB_6 crystals are brought by Joule self–heating which induces switching between its surface– and bulk–dominated conduction. Both states are made unstable by a capacitance C (external or self–capacitance of SmB_6) that is charged and discharged as the sample evolves between different conduction regimes. The oscillations follow, in general, the model of Ref. [17]; they do not depend on the geometry of the crystals although larger contact spacing generally leads to lower oscillation frequencies. A threshold and a maximum value of the bias current and of external capacitance exist between which the oscillations take place; they disappear as the temperature goes beyond 5 K (see Supplementary Material) [19].

In our millimetre–order size crystals, the maximum frequency of self–oscillations at 2 K is of few kHz. It is mostly limited by a time constant of charging/discharging and, therefore, inversely proportional to self–capacitance. A modeling of SmB_6 in the NDR region as an *RC* circuit yields values of 0.1 to 0.5 μF for self–capacitance, depending on the sample size. These values are at least two orders of magnitude larger that the fitted bulk C_b values from low–excitation impedance spectra in the same samples. It suggests then the self–capacitance is related to the surface states. To increase the oscillation frequency, contacting of micro–scale single crystals is clearly desirable.

On the other hand, it is well known that many dissipative systems, such as inductor-capacitor-resistor (*LCR*) circuits with a nonlinear negative–differential resistance show self-sustained oscillations which can be described by the van der Pol equation [25,26]. As shown above, the SmB_6 low-temperature impedance spectra can be interpreted by an equivalent *LCR* circuit, with NDR coming from the self heating. It is therefore reasonable to ask whether the self-sustained voltage oscillations in SmB_6 are the ones depicted by the van der Pol equation. If so, the oscillation frequency should be inversely proportional to the square root of the effective capacitance times inductance, i.e., $LC \propto 1/\omega^2$. This verifies that micro–sized SmB_6 crystals may work as a current-controlled oscillator in the 20 MHz frequency range and above as shown in Refs. [17] and [24].

3.3. Concluding remarks

In-plane and out-of-plane impedance spectra were measured in SmB_6 single crystals in order to study the variation of the dielectric response of this system at low temperatures. A universal model describes quantitatively the complex impedance data in surface- and bulk–conduction dominated regimes. The model includes a R_bC_b circuit and an inductive R_sL_s branch in parallel. The latter becomes dominant at high frequencies. The R_bC_b element is made of a resistor and a capacitor connected in parallel. It describes standard dielectric relaxations in bulk. The R_sL_s branch accounts for the inductive contribution seen below 5 K, in the surface–conduction metallic regime. The equivalent inductance, obtained from fits to experimental data, varies nearly linearly with the surface area at 2 K. It drops drastically with increasing temperature as the bulk starts to control electrical conduction. We tentatively attribute this inductive contribution to the coupling of surface and bulk conduction channels at low temperatures, likely through defects.

SmB_6 single crystals show current–controlled negative–differential resistance at low temperatures, which is brought by Joule self–heating. For reduced samples, self–sustained oscillations of voltage appear across crystals upon biasing with a *dc* current. Their frequencies are limited by the SmB_6 self–capacitance, apparently coupled to the surface states. It is therefore feasible to design and develop devices using micro–crystals of SmB_6. These devices, like oscillators (chaotic and periodic), small signal amplifiers or threshold switches, would benefit a number of important emerging applications, in particular neuromorphic computing.

Declaration of Competing Interest

The authors declare that they have no known competing financial interests or personal relationships that could have appeared to influence the work reported in this paper.

Data availability

Data will be made available on request.

Acknowledgment

We acknowledge the financial support of Ministerio de Ciencia, Innovación y Universidad of Spain through Grant RTI2018-098537-B-C22 co–funded by ERDF, EU. The work at the University of Warwick was supported by EPSRC, UK, through Grant EP/T005963/1.

Supplementary material

Supplementary material associated with this article can be found, in the online version, at 10.1016/j.materresbull.2022.112105

References

[1] M. Dzero, K. Sun, V. Galitski, P. Coleman, Phys. Rev. Lett. 104 (2010) 106408.
[2] T. Takimoto, J. Phys. Soc. Jpn. 80 (2011) 123710.
[3] M. Dzero, K. Sun, P. Coleman, V. Galitski, Phys. Rev. B 85 (2012) 045130.
[4] V. Alexandrov, M. Dzero, P. Coleman, Phys. Rev. Lett. 111 (2013) 226403.
[5] N. Xu, X. Shi, P.K. Biswas, C.E. Matt, R.S. Dhaka, Y. Huang, N.C. Plumb, M. Radović, J.H. Dil, E. Pomjakushina, et al., Phys. Rev. B 88 (2013) 121102(R).
[6] D.J. Kim, S. Thomas, T. Grant, J. Botimer, Z. Fisk, J. Xia, Sci. Rep. 3 (2013) 3150.
[7] M.M. Yee, Y. He, A. Soumyanarayanan, D.-J. Kim, Z. Fisk, J.E. Hoffman, ArXiv e-prints (2013).1308.1085
[8] X. Zhang, N.P. Butch, P. Syers, S. Ziemak, R.L. Greene, J. Paglione, Phys. Rev. X (2013) 011011.
[9] S. Wolgast, c. Kurdak, K. Sun, J.W. Allen, D.J. Kim, Z. Fisk, Phys. Rev. B 88 (2013) 180405(R).
[10] W.A. Phelan, S.M. Koohpayeh, P. Cottingham, J.W. Freeland, J.C. Leiner, C. L. Broholm, T.M. McQueen, Phys. Rev. X 4 (2014) 031012.
[11] N. Wakeham, P.F.S. Rosa, Y.Q. Wang, M. Kang, Z. Fisk, F. Ronning, J.D. Thompson, Phys. Rev. B 94 (2016) 035127.
[12] N.J. Laurita, C.M. Morris, S.M. Koohpayeh, P.F.S. Rosa, W.A. Phelan, Z. Fisk, T. M. McQueen, N.P. Armitage, Phys. Rev. B 94 (2016) 165154.
[13] B.S. Tan, Y.-T. Hsu, B. Zeng, M.C. Hatnean, N. Harrison, Z. Zhu, M. Hartstein, M. Kiourlappou, A. Srivastava, M.D. Johannes, et al., Science 349 (2015) 287.
[14] J. Stankiewicz, M. Evangelisti, P.F.S. Rosa, P. Schlottmann, Z. Fisk, Phys. Rev. B 99 (2019) 045138.
[15] L. Jiao, S. Rössler, D. Kasinathan, P.F.S. Rosa, C. Guo, H. Yuan, C.X. Liu, Z. Fisk, F. Steglich, S. Wirth, Sci. Adv. 4 (2018) eaau4886.
[16] D.J. Kim, T. Grant, Z. Fisk, Phys. Rev. Lett. 109 (2012) 096601.
[17] A. Stern, D.K. Efimkin, V. Galitski, Z. Fisk, J. Xia, Phys. Rev. Lett. 116 (2016) 166603.
[18] M.C. Hatnean, M.R. Lees, D.M. Paul, G. Balakrishnan, Sci. Rep. 3 (2013) 3071.
[19] See Supplemental Material for contact effects in impedance measurements and for more information on voltage oscillations.
[20] E. Barsoukov, J.R. Macdonald, Impedance spectroscopy: Theory, experiment, and applications, John Wiley and Sons Inc., Hoboken, New Jersey, 2005.
[21] J.R. Macdonald, Impedance spectroscopy, Wiley, New York, 1987.Dielectric Relaxation in Solids, Chelsea Dielectrics, London, 1983
[22] A. Jash, S. Ghosh, A. Bharathi, S.S. Banerjee, Phys. Rev. B 101 (2020) 165119.
[23] K.J. Xu, M. Barber, E.Y. Ma, J. Xia, M.C. Hatnean, G. Balakrishnan, J. Zaanen, Z.X. Shen, 2021, ArXiv:2106.00112.
[24] B. Casas, A. Stern, D.K. Efimkin, Z. Fisk, J. Xia, Phys. Rev. B 97 (2018) 035121.
[25] R.H. Rand, Lecture notes on nonlinear vibrations, version 53, Cornell University, New York, 2012.(https://hdl.handle.net/1813/28989)
[26] B. van der Pol, Philos. Mag. Ser. 7 (2) (1926) 978.